SP-1238
March 2000

X-ray Evolving-Universe Spectroscopy - The XEUS Science Case

European Space Agency
Agence spatiale européenne

Prepared by the XEUS Astrophysics Working Group (XAWG):

Monique Arnaud, CEA, Saclay, France
Xavier Barcons, CSIC-UC, Santander, Spain
Didier Barret, CESR-CNRS/UPS, France
Alain Blanchard, Strasbourg, France
Hans Böhringer, MPE, Garching, Germany
Massimo Cappi, TESRE, Bologna, Italy
Andrea Comastri, Bologna Observatory, Italy
Thierry Courvoisier, Geneva, Switzerland
Andy Fabian, IoA, Cambridge, UK
Richard Griffiths, Carnegie Mellon University, USA
Günther Hasinger, AIP, Potsdam, Germany (Chair)
Giuseppe Malaguti, TESRE, Bologna, Italy
Keith Mason, MSSL/UCL, United Kingdom
Takaya Ohashi, Tokyo Metropolitan University, Japan
Frits Paerels, SRON, The Netherlands
Arvind Parmar, ESA/ESTEC, The Netherlands
Luigi Piro, IAS, Roma, Italy
Jürgen Schmitt, University of Hamburg, Germany
Michiel van der Klis, University of Amsterdam, The Netherlands
Martin Ward, University of Leicester, United Kingdom

Published by : ESA Publications Division
ESTEC, PO Box 299
2200 AG Noordwijk
The Netherlands
Editor: Bruce Battrick
Layout: Eva Ekstrand

ISBN No.: 92-9092-548-5
Printed in: The Netherlands
Price: 25 DFl / 10 Euros

X-ray Evolving-Universe Spectroscopy - The XEUS Science Case

1 Introduction

In the first decade of the 21st century, new vistas in X-ray astrophysics will undoubtedly emerge with the advent of the latest X-ray observatories Chandra, XMM and Astro-E. Given the long lead times for major next-generation space astronomy missions, arising from the substantial technological advances required, now is the time to assess the prospects for X-ray astrophysics that will remain when the operational lives of the above powerful observatories end in around ten years' time. The answer is relatively straightforward: cosmology and the unique role that X-ray observations will play in the coherent study of the properties of the evolving Universe.

Assuming the successful completion of the Planck Surveyor and MAP missions in terms of high-resolution mapping of the temperature fluctuations in the cosmic microwave background, major progress is to be expected in the next decade in understanding the evolution of the geometry and density of the early Universe. An in-depth and coherent study of the subsequent formation and evolution of structures in the Universe will require a 'dual-track' observational approach, with complementary studies of the properties of both the *cool* and *hot* baryonic matter components. This scenario is depicted in Figure 1. Cold Dark Matter (CDM) models for hierarchical structure formation predict that primordial fluctuations in the dark-matter density grow and become non-linear, allowing small structures, consisting of both baryonic and dark matter, to collapse first. If the baryon clouds cool and lose sufficient kinetic energy, they become self-gravitating. The collapse of cool dense regions may result in the formation of stars, or gravitationally bound protostellar systems, possibly as early as $z = 10 - 30$, and galaxy formation will follow. Almost certainly this will occur beyond $z = 5$ (Fig. 1).

The formation of structure on the stellar/galaxy mass scale will be probed in the infrared and submillimetre domains with, for example, NGST, FIRST and ALMA. However, it is becoming increasingly apparent that the first formation of super-massive black holes ($M_{BH} \sim 10^5 - 10^7\ M_\odot$) constitutes an integral feature of the galaxy formation process, and that the first black holes also originate at high redshift, i.e. possibly beyond $z = 10$, but certainly at $z > 5$ (Fig. 1, red panels). These black holes could play a very important role in the structure, formation, and thermal history of the Universe by providing a significant fraction of the radiation to ionise the intergalactic medium. High-redshift black holes in their growth phase will be difficult to detect in bands other than X-rays due to their faintness and lack of contrast with other objects and their host galaxy, as well as likely obscuration in that galaxy. X-rays will, however, shine through the absorber and dominate. The

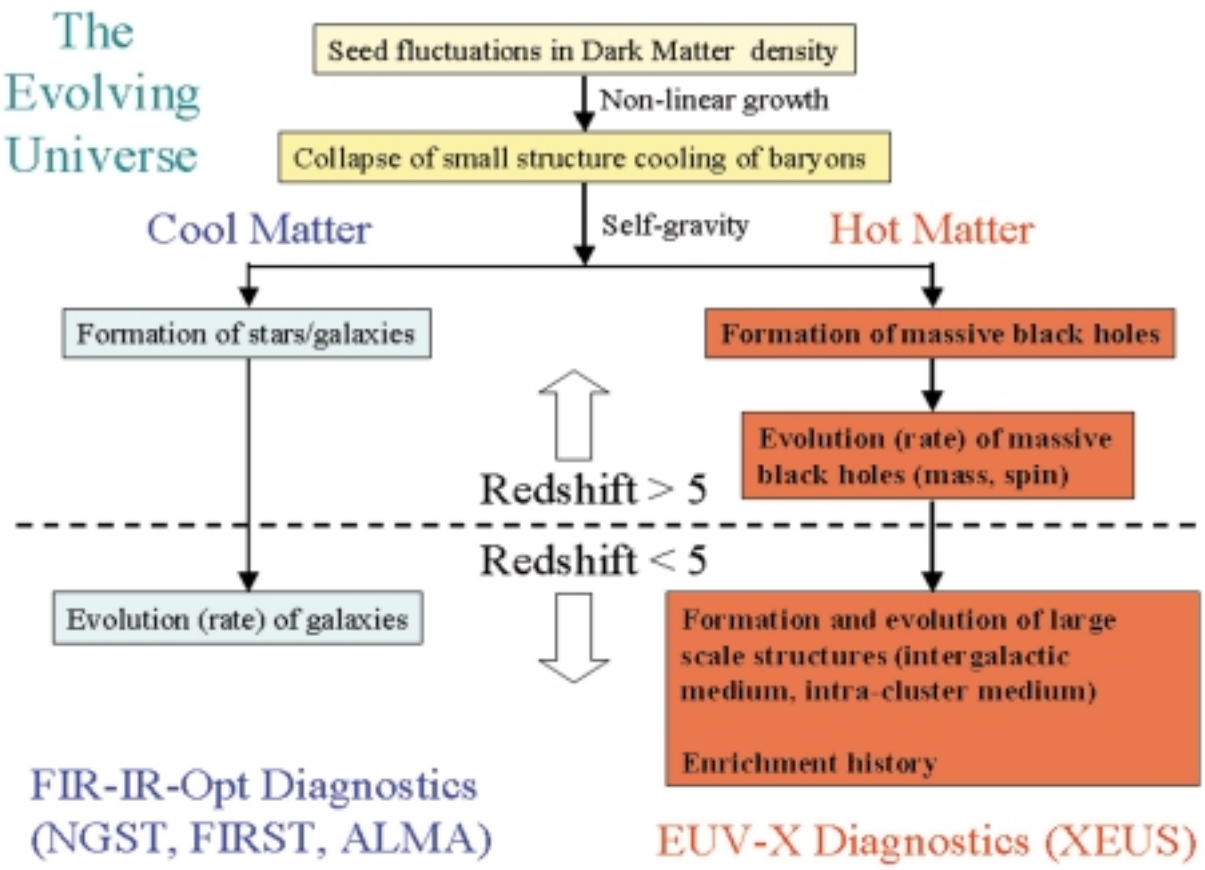

Figure 1. The cold and hot phases of the evolving Universe

only way to discover these first holes, which can have X-ray luminosities in the range $10^{43} – 10^{44}$ erg s^{-1}, and to study their growth and evolution with redshift, is through X-ray spectroscopy. The spin history of black holes will tell us how they have formed and grown.

X-ray spectroscopy is also an essential tool for addressing structure formation on much larger scales than individual galaxies. This is amply evidenced by studies of the hot intra-cluster gas in rich clusters of galaxies in the local Universe, where the hot gas represents more than twice the baryonic matter of all the cluster galaxies, down to the mass scale of hot galactic halos. Models of structure formation in the Universe, starting from the seed inhomogeneities, indicate that the major fraction of matter in the present Universe is hot, with temperatures in the range $10^5 – 10^7$ K (e.g. Ref. 6). The luminosity/temperature relation for clusters and groups of galaxies indicates that a significant amount of additional heat may have been injected into the intergalactic medium, making the Universe even hotter[12]. The, potentially dominant, hot-matter component evolves simultaneously with the cool matter detected in the infrared and submillimetre domains, and can only be traced through high-resolution X-ray spectroscopy, both in emission and through absorption features observed against luminous background sources.

The major goals for a post-Chandra/XMM/Astro-E X-ray astrophysics mission can be summarised as:

- Study the formation of the first gravitationally bound, dark-matter-dominated systems, i.e. small groups of galaxies, and the tracing of their evolution to the massive clusters existing today. These systems may well constitute the dominant fraction of the current mass density of baryons. This study requires at least the ability to measure prominent X-ray spectral features of a moderately enriched (0.3 solar) small cluster at kT = 1 keV at z > 2.
- Study the evolution of metal synthesis down to the present epoch. Since metallicity is very sensitive to local density contrasts, a large spread in metallicity is to be expected at a particular redshift for individual systems. The tenuous hot Intra-Cluster Medium (ICM) is substantially less sensitive to this density contrast and X-ray spectroscopy would appear to provide a much more robust probe of the chemical evolution of the Universe. Note that metal line absorption spectroscopy of the Ly-ALPHA forest only probes the intrinsically metal-poor low-density phase. To assess the enrichment history properly, statistical variations at a given redshift should be averaged out, i.e. the spectroscopic sensitivity of the telescope should allow coverage of a large number of target fields on an almost routine basis.
- Characterise the mass, density, temperature and metallicity of the true Inter-Galactic Medium (IGM). The IGM is most likely dominated by a hot (10^5 – 10^7 K) filamentary structure. Appropriate background sources for absorption spectroscopy comprise high-redshift luminous quasars, and the X-ray afterglows of gamma-ray burst sources.
- Detect massive black holes in the earliest Active Galactic Nuclei (AGN) and estimate their mass and spin. Significant constraints on the origin and growth of massive black holes can only be derived if observations probe the population at z > 4 – 5. This imposes an important design constraint on the effective area of the telescope through the requirement that it be able to detect the relativistically broadened Fe-K emission lines in very distant sources.

The above stated science goals can be met with the following key observatory characteristics:

- A spectroscopic area > 20 m^2 below 2 keV.
- An angular resolution of 2 – 5 arcsec, sufficient to minimise the effects of both source confusion and the diffuse galactic X-ray background.
- A spectral resolution of 2 eV, sufficient for a photon-limited detection of the most prominent emission lines, i.e. O VII, Si XIII and Fe XXV against the sky background and source continuum.

In conclusion, a coherent and complete physical characterisation of the evolution of matter in the Universe requires X-ray spectroscopic diagnostics as an essential element. The present XEUS concept, embodied in a staged and evolutionary development of a large, permanent X-ray telescope facility, meets this challenge in an optimum and highly cost-effective way.

2 The Evolving Universe Seen in X-rays

2.1 Introduction

Modern cosmology and astrophysics are currently addressing fundamental questions such as the origin and the evolution of the Universe:

- What was the physics of the very early Universe?
- What is the nature of dark matter?
- What were the first discrete objects in the Universe - stars or black holes?
- How did galaxies form and evolve?
- How did the large-scale structure, from the first discrete objects to superclusters, form?
- What is the history of the baryons in the Universe?
- How and when were the heavy elements created?

The astrophysics of the 21st century will largely concentrate on the study of the high-redshift Universe, linking the evolution of a diversity of objects and structures to their present-day descendants. Different fields of astrophysics, such as stellar evolution, stellar formation, interstellar medium, galaxy evolution, etc. and different observing techniques in different wavebands will be combined to study cosmology. Ambitious future missions and observatories will study the evolution of the cool and cold Universe: MAP and the Planck Surveyor Mission will measure the cosmological parameters, the amplitude and shape of the primordial fluctuations and will provide a deep insight into the physics of the very early Universe. NGST, FIRST and ALMA will probe the time when the first stars emerged and provide information about the formation and evolution of galaxies.

In the last decades, X-ray astronomy has become an integral part of astrophysics. X-rays provide unique information on a wide variety of astrophysical phenomena, which is complementary to that obtained in other regions of the electromagnetic spectrum. The last few years have seen discoveries that could only have been be made in X-rays: high-energy phenomena around comets in the Solar System, coronal activity from brown dwarfs, young and very nearby supernova remnants, isolated neutron stars, the action of strong gravity in the immediate vicinity of super-massive black holes, the evolution in properties of clusters of galaxies and, finally, the resolution of the X-ray background and its relation to the accretion history of the obscured Universe. The major new X-ray observatories XMM (ESA), Astro-E (Japanese/US) and Chandra (NASA) are providing a significant expansion in the sensitivity limits of X-ray observations, and for the first time enable sensitive high-resolution X-ray spectroscopy of nearby objects.

Large, sensitive X-ray facilities are obviously necessary to study the hot Universe at high redshift. X-rays are produced where and when strong gravity is acting, either in the form of deep or very extended potential wells. There is no better way to trace gravity than with an X-ray telescope. X-ray observations will ultimately provide information about the creation of the first black holes and are the only means of acquiring information on the strong gravity field in the immediate vicinity of a black hole. X-rays are able

to pierce through obscuring gas and dust clouds in the centres of young galaxies and so can disentangle the ambiguity between star-formation and accretion power in the evolving Universe. X-rays will yield essential information on the gaseous and dark-matter components, which are the major contributors to the mass budget of the Universe. Dark matter, which so far can only be studied through its gravitational action on visible matter, can be probed through the evolution of large-scale structures, traced by hot X-ray-emitting gas trapped in the dark-matter potential. However, it is also important to understand the fate and distribution of ordinary matter – the baryons of which we all are made – as a function of cosmic time. Most of the baryons at intermediate to low redshifts ($z < 1$) are probably in the form of warm to hot gas ($10^5 < T < 10^K$) in unvirialized regions, such as the filaments and sheets between superclusters. These can probably only be detected by sensitive soft-X-ray observations. Crucial diagnostics of the chemical and thermodynamic history of the Universe are provided by the abundance and energy content of the Intergalactic Medium, as measured in a straightforward way with X-ray spectroscopy.

We are therefore studying an X-ray observatory for the next millennium, designated XEUS (X-ray Evolving Universe Spectroscopy), which will be able to address the following questions:
– When and how did black holes form?
– How is black-hole evolution related to star formation?
– What is the fate of baryons in the Universe?
– When and how were the heavy elements produced?

XEUS will reveal the cosmic history of the warm and hot Universe.

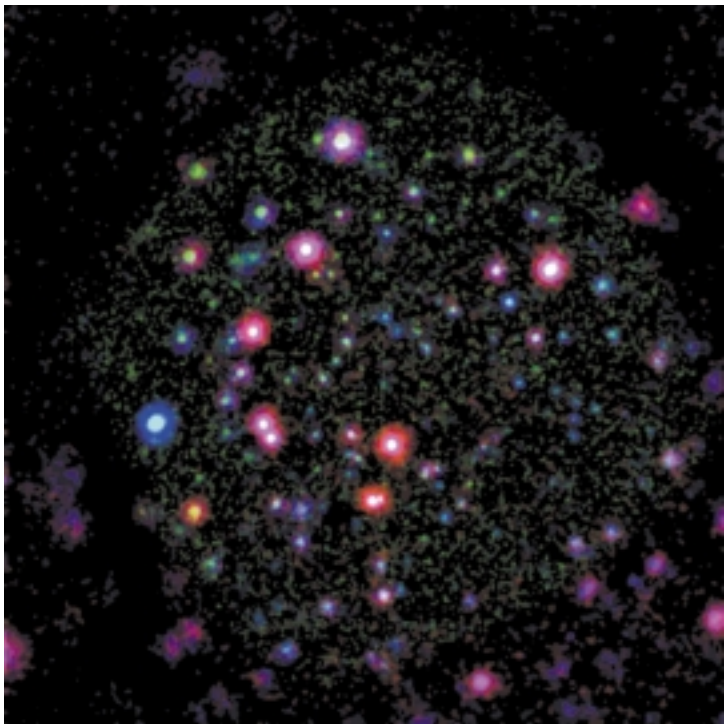

Figure 2. The deepest X-ray image of a serendipitous field so far obtained. The ROSAT PSPC/HRI ultra-deep survey in the Lockman Hole. About 80% of the X-ray background is resolved into discrete sources, which are almost completely optically identified, mainly as Active Galactic Nuclei (AGN). The highest redshift object is an AGN at z = 4.45. (From Ref. 18).

2.2 The first black holes

The cold dark-matter models of hierarchical structure formation predict that primordial fluctuations in the dark-matter density grow and become non-linear. In this scenario, small structures, consisting of baryons and dark matter, collapse first. A discrete object such as a star cluster or a massive black hole can only form if the baryonic clouds can cool efficiently so that they lose sufficient kinetic energy and become self-gravitating. In the early Universe, the cooling is dominated by molecular hydrogen as long as the H_2 molecules are not photo-dissociated. Detailed calculations[43] show that first discrete objects with a baryon mass of ~$10^{5\text{-}7}$ $M_\odot$ can form at redshifts of between 30 and 10 (see Fig. 3). It is unclear what fraction of these objects will turn into early star clusters and into massive black holes[42]. However, the fact that very luminous AGN ($L_X > 10^{46}$ erg s^{-1}) are present at redshifts of z = 5 (see Fig. 2) and that there does not seem to be a substantial decrease of the X-ray AGN space density out to this redshift (see Fig. 4) implies that there are black holes at earlier epochs.

One of the most important open questions about the thermal history of the Universe is whether the intergalactic medium at z > 5 was ionised by stars or by AGN. In the latter case, the ionisation geometry could also have influenced the structure formation. If AGN form at redshifts 20 – 10, they should have black-hole masses of order $10^{6\text{-}7}$ $M_\odot$, corresponding to X-ray luminosities in the range $10^{43\text{-}44}$ erg s^{-1}. An AGN with $L_X = 10^{43}$ erg s^{-1} and a canonical X-ray spectrum with an energy index of -1 at redshifts of 20 and 10, yields an X-ray flux of 2.5 times 10^{-18} and 10^{-17} erg cm^{-2} s^{-1}, respectively. A goal for the XEUS sensitivity is therefore to be able to detect these low-luminosity AGN out to z = 20 and to take spectra of similar AGN to z = 10. Heavily obscured objects at high redshift are accessible in the X-ray range because the redshift produces a 'negative k-correction', shifting the unobscured high-energy part of the spectrum into the observable domain.

Detailed iron-line spectroscopy and time-variability analysis will constrain the physical properties and the chemical composition of matter in an accretion disk in the immediate vicinity of the black-hole event horizon, as well as the mass and possibly the spin of the black hole. Statistics over a large number of AGN at different redshifts will thus yield the evolution of black holeís mass and spin rate. This can be directly compared with the evolution in number density and luminosity in order to obtain information on the accretion physics of these early objects. The spin history of black holes may directly tell us about the way in which early black holes grow, since continuous accretion will yield a high spin rate, while mergers of larger black holes will produce an intermediate or low spin rate.

2.3 The absorbed high-redshift Universe

Global properties of the optical and UV Universe as a function of cosmic time suggest that star formation and metal production peaked at a redshift around 1 – 2 (Ref. 24). These results, however, may have to be significantly revisited because of the unknown role of absorption at high redshifts. This

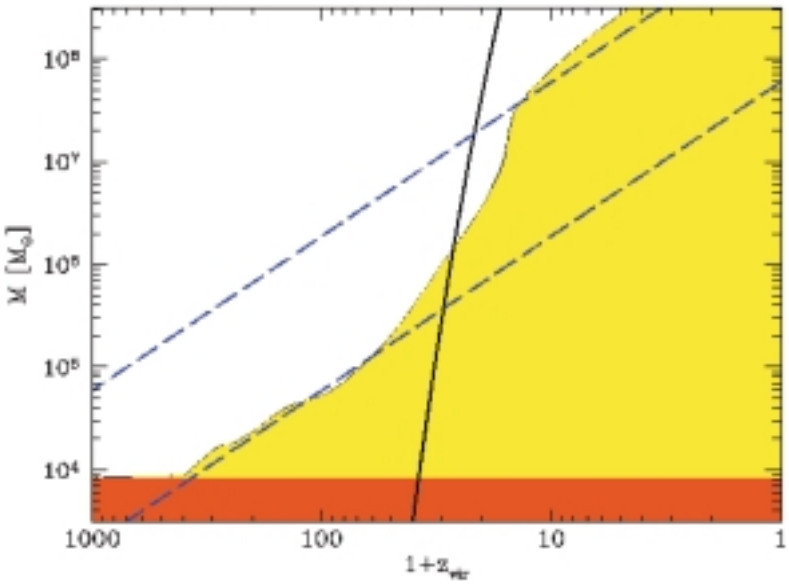

Figure 3. The minimum mass of dark halos needed to form discrete objects in the early Universe. Haloes with masses above the light shaded area (yellow) can collapse and form luminous objects. The dashed straight lines corresponding to virialization temperatures of 10^3 and 10^4 K are shown for comparison. Objects in the dark shaded area (red) can never collapse, because their virialization temperature would be below that of the cosmic background field at that redshift. The solid line corresponds to 3σ peaks in a standard CDM model, normalised to $\sigma_8 = 0.7$, such that objects of halo mass 2 x 10^6 $M_\odot$ can form at z = 30. If black holes form at z = 10 - 20, they can have X-ray luminosities in the range $L_X = 10^{43-44}$ erg s^{-1}. (From Ref. 43).

affects the results in two ways. Firstly, neglecting dust absorption may lead to an underestimation of the real star-formation rate[33] and, secondly, it is possible that a population of heavily dust-enshrouded high-z objects may have escaped detection in optical/UV surveys[3]. Indeed, deep submillimetre surveys with SCUBA have revealed the existence of a large population of hitherto undetected dust-enshrouded galaxies[21]. These sources are believed to be the high-z equivalent of the local Ultra-Luminous Infra-Red Galaxies (ULIRGs). A local example of such a source is NGC 6240, which has a heavily absorbed active nucleus, detected by BeppoSAX[44], embedded in an exceptionally powerful starburst.

Although the abundances of optically and radio-bright quasars declines at $z \geq 2.5$ (Ref. 40), simple cosmological models for hierarchical structure formation reproduce the decline, but simultaneously predict a substantial population of (optically) faint quasars at larger redshifts. It is thus possible that the low optical emission efficiency of these quasars is due to obscuration by dust, and thus X-rays are the preferred way to probe their true nature[14]. As shown in Figure 4, preliminary direct evidence for such a population is indicated by the latest ROSAT X-ray results[18], which show a constant quasar density from z = 2 to 4.

Deep soft-X-ray surveys carried out with ROSAT have resolved a significant fraction (70 – 80%) of the soft X-Ray Background (XRB) into discrete sources. Optical identification follow-up results indicate that the great majority of the faint ROSAT sources are AGN, which are thus the major contributors to the soft XRB. At higher energies, the shape of the X-ray background spectrum and the source counts can be reproduced assuming a population of heavily obscured AGN[41]. Indeed, X-ray observations with ASCA and BeppoSAX have clearly established that many, heavily obscured, AGN are present in the local Universe, with column densities as high as $\geq 10^{23-24}$ cm^{-2} (e.g. Ref. 27), lending further support to the AGN synthesis models for the XRB. According

to detailed models[7], the most important contribution to the XRB energy density is provided by sources with column densities of the order of $10^{23\text{-}24}$ cm^{-2}, relatively high 2 – 10 keV luminosities (~$10^{43\text{-}45}$ erg s^{-1}), and typical redshifts in the range z = 1 – 3, or more. As a result, a large fraction of the Universeís high-energy output is obscured[11]. Even if the model predictions are extremely uncertain because the space density and cosmic evolution of obscured sources are essentially unknown, it is clear that only extremely deep X-ray observations will reveal the nature of the sources that dominate the Universe's high-energy output. In order to study the history of the accretion-powered obscured Universe, high-quality X-ray spectra of a sizeable sample of high-redshift objects are needed. This goal is beyond the capabilities of the foreseen deep Chandra and XMM surveys. The expected number counts of absorbed AGN as a function of redshift is plotted in Figure 4. A good sampling of the high-z tail of the redshift distribution can be obtained only for 2 – 10 keV fluxes of the order 10^{-16} erg cm^{-2} s^{-1}. These fluxes will be reached in a reasonable exposure time by XEUS, as detailed below.

2.4 Structure formation and the history of heavy-element enrichment

X-ray astronomy permits the study of the hot baryonic matter component within the large-scale structure of the Universe. In particular, it allows the

Figure 4. Left: Cosmic star formation history τ_{SFR} (left Y-axis) compared to the space density ϕ of luminous X-ray-selected AGN (right Y-axis). Filled circles give the co-moving number density of ROSAT AGN with $L_X > 3 \times 10^{44}$ erg s^{-1} (Ref. 29). Open circles give the optical/UV measurements of the star-formation rate from Reference 3. The dashed line indicates the simplest star-formation history model of Reference 3, which explains the whole far-infrared/sub-mm background light by dusty star formation. Note the similarity between this model and the quasar space density. (From Ref. 18).
Right: The number counts of highly obscured sources (with 10^{42} erg s^{-1} < $L_{2\text{-}10}$ < 10^{47} erg s^{-1} in three redshift intervals computed assuming the same X-ray luminosity function and evolution of unabsorbed quasars. The vertical lines represent the limiting sensitivity of XEUS with different configurations and exposure times.

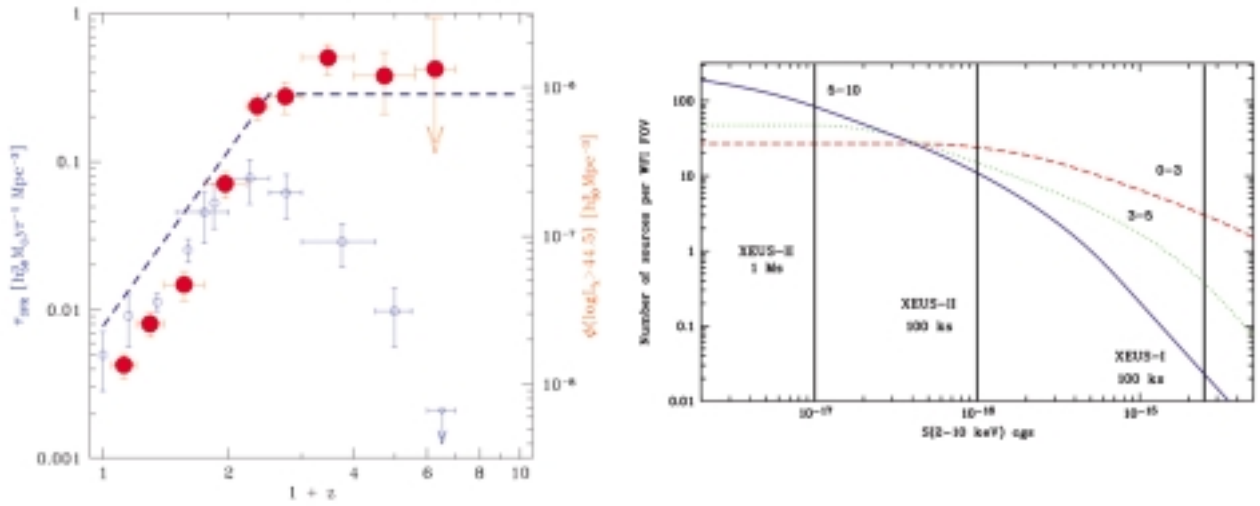

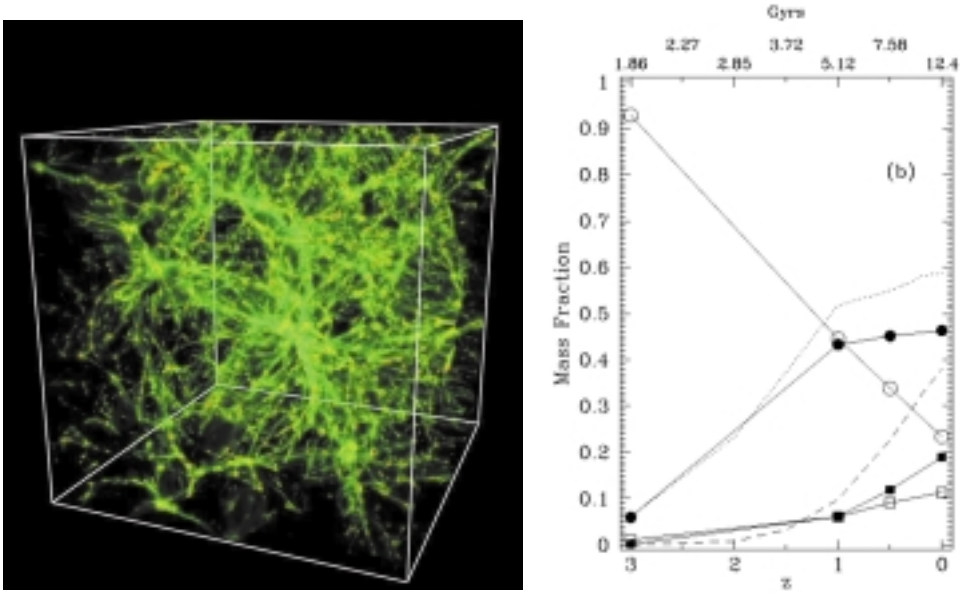

Figure 5. Left: Spatial distribution of the warm and hot gas with temperatures in the range $10^{5\text{-}7}$ K at z = 0, which according to hydrodynamic simulations[6] is the most abundant form of baryons in the local Universe.
Right: Mass fraction of baryons of different temperature as a function of redshift. Open circles are baryons of temperature < 10^5 K, filled circles of temperature $10^{5\text{-}7}$ K and filled squares of temperature T >10^7 K. Open squares refer to baryons in galaxies. (From Ref. 6).

hot plasma bound to the gravitational potentials of the largest mass aggregates in the Universe to be traced: the groups and clusters of galaxies. These studies have provided some of the most exciting information used to test cosmological models: e.g. the ratio of presumably non-baryonic 'dark matter' to the baryonic component of the Universe[45], an illustration of how large objects are formed through the hierarchical merging of smaller units[20], the high iron and other heavy-element pollution of intergalactic space, implying a much more violent starburst history than previously assumed[1], and the mapping of the cosmic matter distribution on the very largest scales[4].

These studies have mainly provided information on the present state of the Universe, with little observational evidence for evolution. The large effective area and the high angular resolution of XEUS will enable these very successful studies to be extended to high redshifts to study groups and clusters of galaxies at the epoch when these most massive objects first emerged, and when the pollution of intergalactic space by violent starbursts and galactic winds was presumably at its peak at redshifts around 2 - 4.

The majority of the baryons in the Universe are probably outside the most prominent discrete structures and their radiation is therefore too faint to be detected. However, absorption features against a bright background source can make them visible, as is well known from classical Ly-α forest spectroscopy. If their temperature is >10^5 K, the corresponding absorption features lie in the X-ray range.

When and how do massive structures form?

In the standard cosmological scenario of hierarchical structure formation, bound objects are formed from the collapse of initial density fluctuations that grow under the influence of gravity. Small structures form first and grow into larger objects, both via merger events and by continuous accretion of surrounding matter, mostly along filamentary structures (Fig. 5). From observations with the Planck Surveyor Mission, we will know the initial conditions of this formation process, i.e. the amplitude and shape of the initial fluctuations, as well as the global parameters governing cosmic evolution. Neither the cosmological simulations nor the microwave background observations will yield information about the complicated physics of gas cooling and heating processes governing galaxy formation. Much of this gas is heated to, and cooling from, soft-X-ray emitting temperatures. With XEUS we will be able to understand the physics that governs large-structure formation and evolution. We will:

- Study the first groups forming the 'seeds' of to-day's massive clusters. The epoch when this occurred provides an important point of orientation for the structure evolution with z. Understanding the formation process is a key to understanding the properties of present-day clusters and their galaxy population.
- Understand the role of feedback from the cluster galaxies to the physical and chemical state of the gas at high z. The dynamical and thermodynamical evolution of the intra-cluster medium is not purely governed by gravitational effects. Galaxies are injecting metals and energy, probably at early epochs through supernova-driven winds, and this feedback from galaxies is likely to affect cluster formation and evolution. In addition, central cooling in the early dense groups and cluster cores can have an important effect on the evolution. Such 'cooling flows' have been proposed to be very prominent at high z and may be responsible for triggering quasar activity in central groups or clusters of galaxies.
- Test the hierarchical formation scenario from merging activity at high z and the evolution of sub-clustering with z. Mergers of clusters are the most energetic events in the Universe since the Big Bang (~ 10^{63} erg over a time scale of 10^9 years). We will understand the physics of merger events in detail. The collision of two sub-clusters should be manifest by characteristic features in the temperature maps, such as heated gas between the sub-clusters before the collision, as well as steep temperature gradients (increases by a factor of 2 – 3 over typically 200 kpc) at the shocks formed during the collision. The velocities of the gas can range from 200 to 2000 km s^{-1}. XEUS will have the spatial resolution and sensitivity to resolve such shocks in detail, as well as the spectral resolution to measure the mass motion from emission-line spectroscopy.
- Trace the outskirts of clusters and study larger scale structures such as filaments through absorption lines. This will enable us to understand if, and how, clusters continuously accrete intergalactic matter.

Here it is important to understand that the histories of the gas and galaxy formation are deeply interconnected. During galaxy formation, the physical (temperature, density) state and chemical composition of the gas are fundamental in determining the fate of the collapsing gas: whether it can cool or not is critical. Direct information on this gas is unfortunately extremely difficult to obtain. However, in the final state of the gas falling into clusters, its chemical composition and entropy are fossils of its evolution. X-ray studies are the most direct way to obtain information on the gas history, which ultimately controls the overall history of galaxy formation.

What is the cosmic history of heavy-element enrichment?

One of the fundamental astrophysical questions is the cosmic history of heavy-element production and circulation. It is strongly related to several other important issues, such as the history of star formation, the possible variations in the stellar initial mass function with the environment and the circulation of matter between the various phases of the Universe. NGST, FIRST and ALMA will provide essential constraints on the history of the star formation rate. Clusters of galaxies are excellent laboratories with which to study the cosmic history of heavy-element production. They are the largest closed systems where the chemical enrichment process can be studied in detail. Furthermore, X-ray observations of the lines emitted by the hot intra-cluster medium will allow the determination of abundances to much higher redshifts than reachable via optical observations of normal galaxies. X-ray observations have the further advantage that they provide direct measurement of the abundances, without having to rely on the indirect indicators used in the optical for the element abundances in galaxies. Abundance gradients in clusters and groups of galaxies will directly measure the history of the chemical enrichment of the intergalactic medium, much better than is possible using individual galaxies. Cosmic abundances in very poor groups can be determined to any redshift using X-ray absorption-line spectroscopy as long as a bright background source can be found. In the case of gamma-ray burst afterglows, this is also true for the host galaxy and all intervening systems.

XEUS will measure the abundances of all astrophysically abundant elements, down to the photon-limited detection limit: the energy resolution will be much smaller than the equivalent width of the strongest emission lines, over a large range of temperatures. We will thus obtain information on the heavy-element enrichment history of the intra-cluster medium (with implications for the evolution of cluster galaxies) of a quality now only reached for our Galaxy. With XEUS, we will:

- Trace the evolution of the intra-cluster medium abundances back to at least $z \sim 2$ and down to poor clusters. We will thus constrain the epoch of production and ejection of the heavy elements and understand the interplay between the dynamical history (in particular the effect of mergers) and the chemical history of clusters.
- Compare the spatial distribution of heavy elements and galaxies up to

high redshift. This will provide a strong constraint on the ejection process (wind or ram pressure stripping).

– Probe abundances in the intergalactic medium (see also Section 4.5) and check if the metal-production efficiency of field and cluster galaxies is similar to the predictions of current models.
– Measure precisely the α-element over Fe-abundance ratio back to z ~ 2 and thus constrain the relative importance of type-I and type-II supernovae and their past rates. This is a strong constraint on the initial mass function, and also has far-reaching consequences for the thermal history of the inter-cluster medium.
– Provide independent constraints on the star-formation history, since the overall cluster metal content is a fossilised integral record of the past star formation.

3 The XEUS Mission

As detailed in the specific science examples below, a sensitivity to measure the broad-band spectra of sources as faint as ~10^{-17} erg cm^{-2} s^{-1} in the 0.5 – 2 keV energy range and a photometric limiting sensitivity of ~10^{-18} erg cm^{-2} s^{-1}, ~250 times fainter that the ROSAT deep-survey limit[18] will allow some of the most fundamental questions in astrophysics to be addressed. XEUS has been designed to meet these goals. XEUS is a potential follow-on to the recently launched ESA Cornerstone X-ray Multi-Mirror (XMM) spectroscopy mission and is under study, as envisaged by the Horizon 2000 Survey Committee, who recommended analysing the potential offered by a major high-energy astrophysics facility within the Space Station Utilisation Programme. XEUS is planned as a long-term X-ray observatory, which will be grown in orbit. The initial mission configuration, termed XEUS1, will be launched by an Ariane-5 vehicle into a Fellow-Traveller Orbit (FTO) to the International Space Station (ISS). It will consist of a mirror spacecraft, MSC1, with a 1keV effective area of 6 m^2 and a separate

Figure 6. PSFs used for the simulations. The HEWs are 2, 5 and 15 arcsec, respectively, from left to right. The rightmost curve corresponds to the PSF of the XMM qualification mirror module.

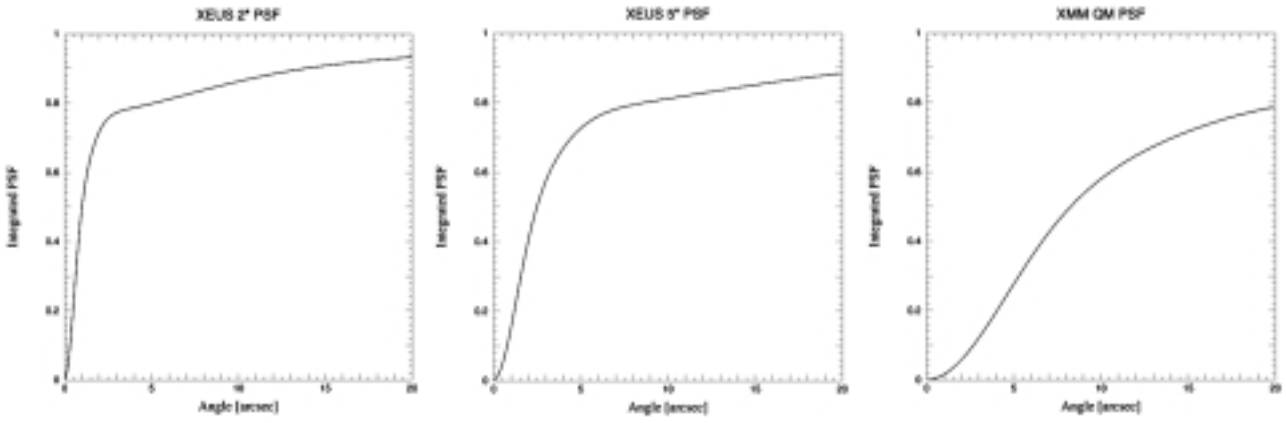

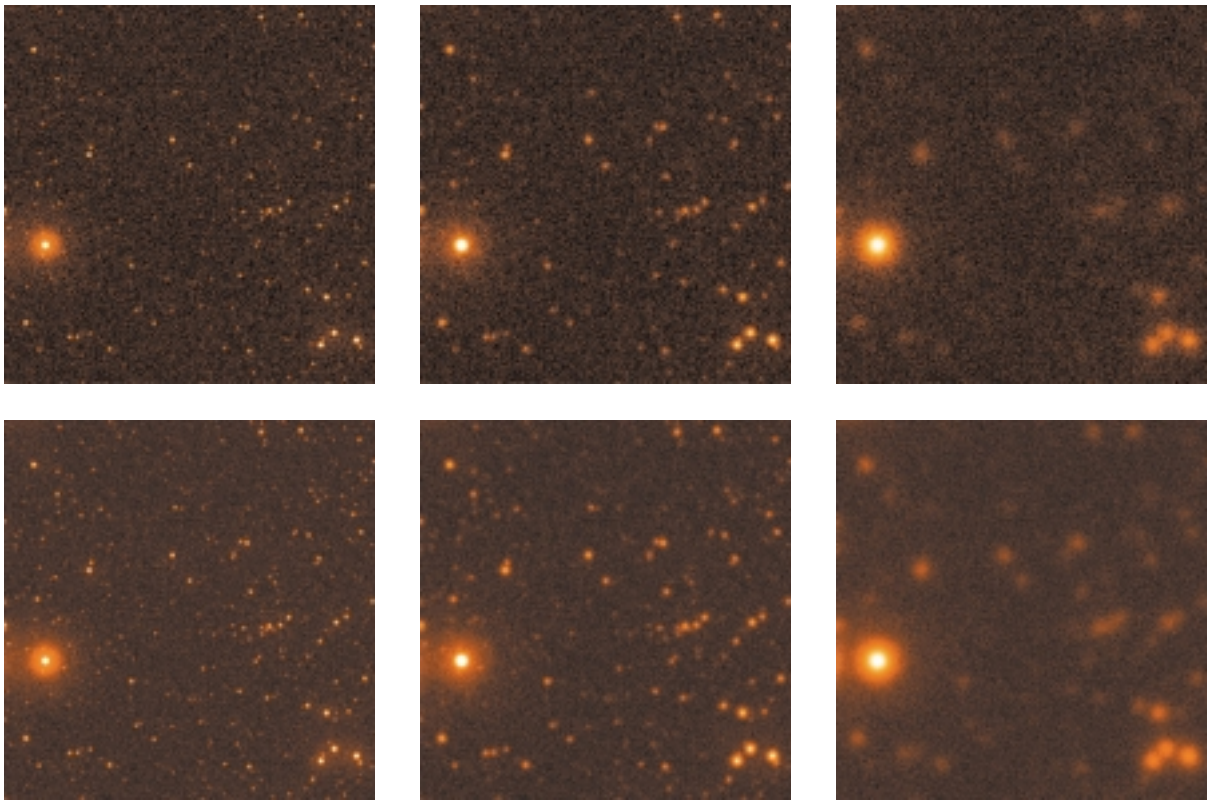

Figure 7. Simulated XEUS images with the WFI. Each image is 5 arcmin square. From left to right, PSFs with HEW of 2, 5 and 15 arcsec, have been assumed, respectively. The upper row is for the XEUS1, the lower one for XEUS2. The 'bright' source at the lower left has a flux of 2 x 10^{-14} erg cm^{-2} s^{-1}.

detector spacecraft, DSC1. The two spacecraft are aligned by active control to provide a focal length of 50 m with an accuracy of 1 mm^3.

After several years of operation, XEUS1 will visit the ISS, where MSC1 will be grown to MSC2 with a 1 keV effective area of 30 m^2 through the robotic addition of extra segments. DSC1 will be replaced by a new detector spacecraft DSC2, with next-generation instruments. The new configuration, XEUS2, will be boosted to FTO and begin operations lasting many years. At 8 keV, the mirror area will be 3 m^2 for both XEUS1 and XEUS2. XEUS will be sensitive over the energy range 0.1 – 30 keV with a 1 keV spatial resolution of 2 to 5 arcsec. The instrumentation will consist of both narrow- and wide-field imagers, with fields of view of 1 and 5 arcmin and energy resolutions of ~2 eV and ~50 eV at 1 keV, respectively.

3.1 Requirements on mirror area and angular resolution

The X-ray background in the 1.0 – 10 keV energy range is primarily composed of an extragalactic power-law component with an energy slope of 1.4 – 1.5 (Refs. 13 and 28) and a 0.2 – 2.5 keV surface brightness of 9.3 x 10^{-19} erg cm^{-2} s^{-1} $arcsec^{-2}$. This is probably the sum of many discrete sources and should be largely resolved at the faint fluxes considered here. At

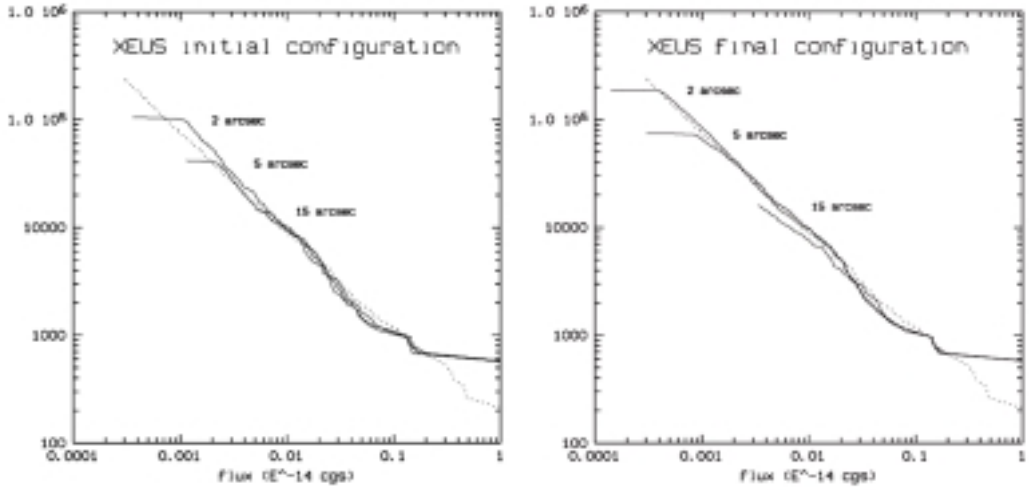

Figure 8. Comparison between the log(N) - log(S) relation on input to the simulations (dotted line) with the detected relation. The left figure compares the output data for the XEUS1 configuration, the right figure for XEUS2.

energies <1 keV, there is additional galactic soft-X-ray emission, which can be described by thermal components with temperatures of 0.08 and 0.25 keV (Refs. 15 and 31). This component varies by a factor of ~ 7 as a function of galactic latitude, and at high latitudes has a surface brightness of 5.6 x 10^{-19} erg cm^{-2} s^{-1} $arcsec^{-2}$. The background flux in an X-ray beam depends on the Half-Energy Width (HEW) of the Point-Spread Function (PSF). For HEWs of 1, 2, 5 and 15 arcsec, the galactic background flux corresponds to 0.04, 0.18, 1.1, and 9.9 x 10^{-17} erg cm^{-2} s^{-1}, respectively, and is of the same order as the signal to be observed. Broad-band XEUS spectroscopic observations will therefore be sky-background limited.

In order to achieve broad-band spectroscopy with a crude characterisation of the spectrum, i.e. to determine a flux, power-law slope and column density, we assume that a signal-to-noise ratio of 30 is sufficient. To reach this ratio with a flux of 10^{-17} erg cm^{-2} s^{-1} in 10^6 sec, an effective mirror area of tens of square metres around 1 keV and a high enough angular resolution to minimise the effects of both the diffuse X-ray background and source confusion are needed. In order to transform these boundary conditions into realistic requirements for the system, simulations were performed with three different realistic PSFs with HEWs of 2, 5 and 15 arcsec (Fig. 6) and two different effective-area configurations, corresponding to the XEUS1 and XEUS2 missions before and after mirror growth.

The simulations were performed in the 0.5 – 2 keV energy range. A log(N) - log(S) according to the ROSAT deep-survey finding[16] as a broken power-law function for the differential source counts was assumed. In this representation, the extragalactic soft-X-ray background is resolved completely at a flux of 2 x 10^{-18} erg cm^{-2} s^{-1} at a surface density of ~10^5 deg^{-2}. The XEUS Wide-Field Imager with a field of view of 5 x 5 $arcmin^2$ has been assumed. Figure 7 shows the six resulting images simulated with

an exposure time of 100 ksec. It is obvious that the images with the smallest PSF are the most sensitive and that those with a 15 arcsec HEW are severely confusion-limited. The simulated exposures have been analysed with a simple map detection algorithm. Figure 8 compares the input and output log(N) - log(S) for the different configurations. The image, using the XEUS2 configuration with the highest angular resolution, yields a limiting sensitivity of 4 x 10^{-18} erg cm^{-2} s^{-1}. The corresponding detected log(N) - log(S) relation is significantly above the input curve at the faintest fluxes, an effect known as the 'Eddington Bias' in an unconfused situation (see Ref. 17). All other log(N) - log(S) relations show significant indications of source confusion at the faint end, the effect of which is dramatic in the case of the 15 arcsec HEW PSF. A mirror resolution as high as possible, ideally 2 arcsec HEW, is therefore required to achieve the highest sensitivity and lowest confusion. A HEW of 5 arcsec is still acceptable, but will imply a significant degradation of sensitivity.

In Figure 9, the spectroscopic sensitivity of XEUS is compared with that of a number of future missions and modern ground-based observatories over the whole electromagnetic spectrum in a $\nu \cdot f(\nu)$ representation. For reference, the spectral energy distributions of a hypothetical 3C273-type quasar at redshifts of 10 and 20 are given as well. A limiting spectroscopic flux of 10^{-17} erg cm^{-2} s^{-1} has been assumed for XEUS. This figure shows that the sensitivity of XEUS is on an equal footing with the most advanced observatories at all wavelengths in terms of emitted energy per decade.

Figure 9. Comparison of the sensitivities of future observatories in different wavebands. A horizontal line corresponds to equal power output per decade of frequency. The following observational conditions have been assumed: ALMA[2]: a large millimetre array with 50 antennas of 10 m diameter, 8 h integration; FIRST[34]: 5σ detection, 1 h exposure, photometry (R = 3; lower curve), spectroscopy (R = 200; middle curve), spectroscopy (R =10^{5-6}; upper curve). VLT: 5σ imaging, FORS UBVR 0.5 h integration, CONICA JHKLM 1 h integration (http://www.eso.org/instruments/). NGST[22] 5σ detection, integration time 10 ksec, photometry (R = 5). XEUS: 100 ksec exposure. Power-law spectrum (0.05 - 30 keV) with a photon index of 2.0 and a 0.5 - 2.5 keV flux of 10^{-17} erg cm^{-2} s^{-1}.

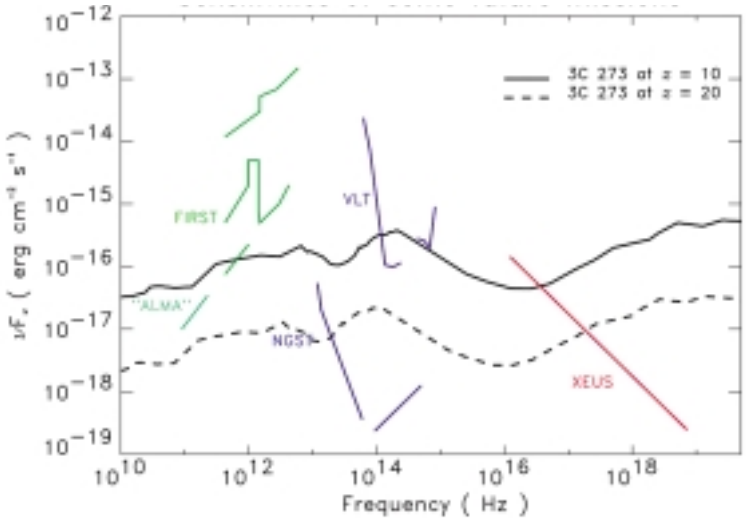

3.2 Requirements on spectroscopic sensitivity

Hierarchical clustering and chemical evolution

One of the major goals for XEUS, and its most exacting design driver, is the detection and characterisation of groups and clusters of galaxies, from their first appearance at cosmologically significant redshifts, down to the present epoch. This implies a set of requirements on the *spectroscopic* sensitivity of the observatory, because: (i) of the need to directly measure the redshifts of the candidate groups from the X-ray data (these objects will be too faint for unambiguous optical identification), (ii) in order to do so, at least a few emission lines will have to be uniquely detected, and (iii) in order to reliably measure such properties as chemical composition, the ability to diagnose non-equilibrium conditions is required.

Examining each of these issues in turn, the first requirement by itself, redshift measurement, is not stringent. At significant redshifts, the relative accuracy does not have to be very high in order to correctly assign a group or cluster to a cosmological epoch. We expect the gas in these objects to be relatively cool (kT_e < 1 keV), and at these low temperatures, the emission spectrum is dominated by Fe-L emission around 700 – 1000 eV. At low resolution and signal-to-noise, measurements of redshift and temperature (or average ionisation) are strongly correlated. This degeneracy cannot be broken unless at least a few emission lines can be uniquely identified. This requirement, of being able to resolve the strongest lines in the Fe-L emission spectra, in itself imposes a lower limit on spectral resolving power of $E/\Delta E > 100$, or $\Delta E < 10$ eV at E= 1000 eV. However, the requirement of being able to detect the strongest emission lines against the sky and instrumental backgrounds and the continuum emission imposes a much more stringent limit of $\Delta E \sim 2$ eV; at this limit, the detection is guaranteed to be photon-limited. Numerically, this argument follows from assuming an average high-latitude galactic background intensity of 2×10^{-6} photons $cm^{-2}\ s^{-1}\ keV^{-1}\ arcmin^{-2}$ at

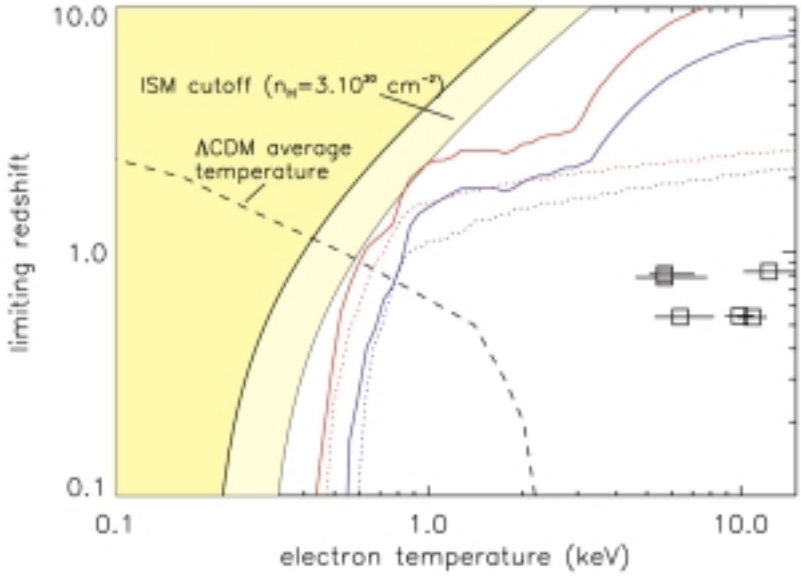

Figure 10. The XEUS sensitivity to the detection of metal emission lines from clusters and groups of galaxies at different redshifts. The lower dotted lines are sensitivity to detecting just the α elements. Red shows the spectroscopic sensitivity of XEUS2 and blue XEUS1. The luminosity/temperature relation of Reference 37 was assumed. The black dashed line shows the emissivity-weighted temperature of the cluster gas, calculated in Reference 6. The data points represent the six most distant X-ray-selected clusters for which a temperature estimate is known[10,30]. The shaded area shows the fraction of the T - z plane fundamentally obscured by absorption in our own Galaxy, assuming a column density of $N_H = 3 \times 10^{20}$ cm^{-2}; the lighter shading indicates the decrease in obscuration associated with a lower column density, of $N_H = 10^{20}$ cm^{-2}.

E ~ 300 eV, and the effective area at 300 eV as currently projected for the XEUS2 configuration (~ 20 m^2). This produces 60 (ΔE / 2 eV) sky-background counts per arcmin diameter FOV in 10^5 sec of exposure time. The instrumental background and continuum counts per resolution element are negligible. More or less arbitrarily limiting the sky background to 25 counts per resolution element (the number that would yield a 5σ detection in a purely source photon statistics limited observation) then suggests a required resolution $\Delta E < 1$ eV. In practice, explicit calculations (see below) show that due to the steep dependence of source flux on redshift, for a fixed luminosity, the sensitivity is optimum as long as $\Delta E \leq 2$ eV.

Given a photon-limited detection, evaluating the largest redshift out to which a group can still be studied spectroscopically is straightforward. Figure 10 shows this limit (joint 5σ detection of the most prominent lines from each abundant element, in 10^5 sec, one-third solar metal abundances) as a function of the plasma temperature of the intra-group medium. The luminosity was set according to the temperature-luminosity relation given in Reference 37, including the steep drop in luminosity below kT ~ 800 eV. The fraction of the cluster light in the field of view was calculated assuming a 250 kpc core radius, and a flat cosmology with $\Omega_{matter} = 0.3$, $H_0 = 75$ km s^{-1} Mpc^{-1}. The detection limits for an extreme composition consisting of H, He, and the α-elements only are also shown.

To put these limiting redshifts into perspective, the part of the kT - z plane fundamentally inaccessible due to absorption in our galaxy is also displayed. This is calculated using $\langle E \rangle \sim kT/(1+z) > 300$ eV (corresponding to the absorption limit imposed by a column density of 3×10^{20} cm^{-2}. This blocks out the coldest and/or most redshifted groups and clusters. XEUS2, in its final configuration, can *spectroscopically* access almost the entire unobscured portion of the kT – z plane, and in a sense will therefore be the definitive X-ray observatory for cluster astrophysics. This indicates that the currently designed effective area is almost perfectly matched to this problem. In fact, due to the very steep dependence of the limiting redshift on source temperature (i.e. luminosity or mass), there is no gain in sensitivity unless the area is increased by almost an order of magnitude.

The same figure also displays the current best available calculation for the (emissivity-) averaged temperature of the Inter-Galactic Medium (IGM)[6]. To indicate the effect of statistical fluctuations on this relation or, possibly, to what extent this calculation is likely to correctly represent the true state of the IGM, the positions of the six most distant X-ray selected clusters for which a temperature estimate is available are also plotted[10,30]. If clusters are also present, at comparable relative frequency, with temperatures far above the average value at larger redshifts as they are locally, XEUS will detect these extreme examples to z = 3.

Finally, we would point out that at the lower temperatures, we significantly detect emission from Fe-L, O VII and O VIII transitions. At higher

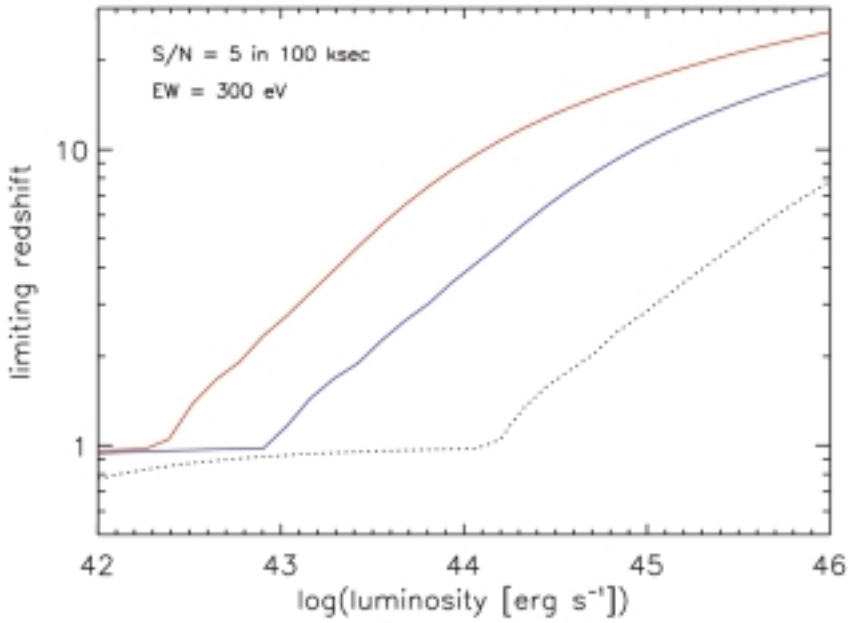

Figure 11. The ability of XEUS, again both the XEUS1 (blue) and XEUS2 (red) configurations, to detect and measure massive black-hole formation in the Universe through the study of the distorted Fe-K lines originating in the strong gravity field in the immediate vicinity of the black hole. The limiting redshift is plotted as a function of AGN luminosity. In the 10^{43-44} erg s^{-1} luminosity range XEUS2 is required to detect an Fe-K line with an equivalent width of 300 eV beyond z = 4 - 5. The dotted line gives the XMM EPIC sensitivity, for comparison.

temperatures, the line emission is dominated by Fe-K transitions together with K-shell emission from the mid-Z elements. At each temperature, we will therefore detect emission from ions with widely separated ionisation potentials, which will enable the spectroscopic investigation of the importance of non-equilibrium effects on the inferred parameters of the clusters, most notably their metal abundances (at large redshift, the dynamical-, ionisation-, and gas-kinetic equilibration time scales are of the same order as the ages of the clusters if the gas densities are below a few times 10^{-4} cm^{-3}).

Early massive accreting black holes

Another major goal for XEUS is to search for early massive black holes using their accretion-driven X-ray emission. The expected strong, relativistically broadened Fe-K line emission will be the signature used to identify black holes, and to obtain an estimate of their redshift. This requires detecting such Fe-K emission line(s) from the inner regions of the accretion disk around the black hole. Since the Fe-K profiles are several keVs wide, this in itself does not require high spectral resolution. Instead, the sensitivity depends on effective area only, for a chosen set of line parameters. Figure 11 shows to what redshift a (rest frame) 300 eV equivalent width (EW) emission line, seen against a canonical AGN continuum, can still be detected at 5σ confidence, as a function of X-ray luminosity. For simplicity, the line profile was assumed to be a square box with a width of 3 keV.

The shape of the Fe-K line does not depend on the mass of the black hole. For local, bright AGN, a measurement of the relevant variability time scales through reverberation mapping may provide the necessary absolute length scale. This information will most likely not be accessible for distant AGN, so

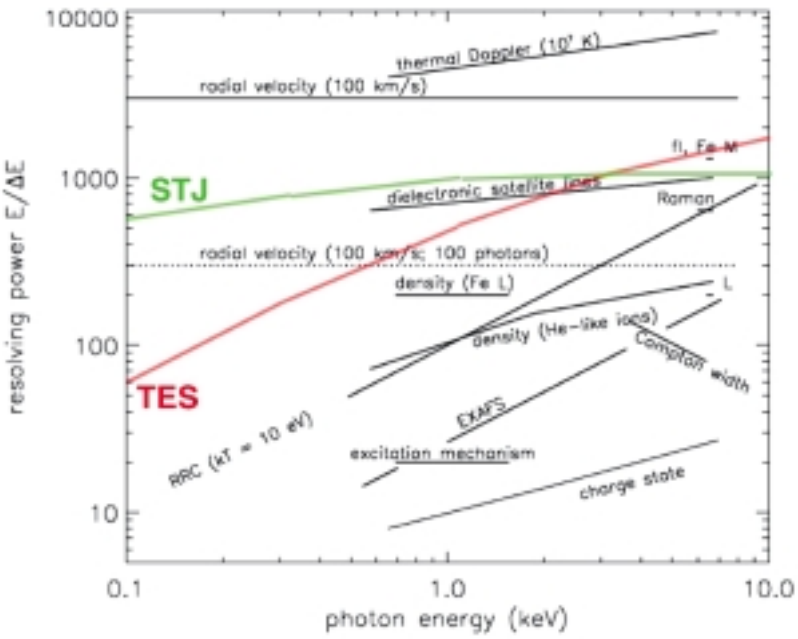

Figure 12. Resolving power necessary for the diagnostics of different physical processes. The assumed resolving power of the two assumed spectroscopic instruments is also given.

that we have to resort to indirect methods to estimate masses. There is a well-known correlation between the black-hole variability time scale and its mass, which could be used in a statistical sense for distant black holes. We can also obtain a lower limit on the mass from the measured luminosity, and the theoretical upper limit on the radiative efficiency. Extreme gravitational redshifts will still provide a measure of the black hole's spin. At sufficiently early times, the time scale for doubling of the mass by Eddington-limited accretion corresponds to an ever-increasing redshift interval. Once we reach $z \sim 4 - 5$, the growth of massive holes must stretch back to very early times, and even a statistical mass estimate or limit will put significant constraints on the initial mass of the holes, the growth rate, and the epoch of formation.

Diagnostics of astrophysical plasmas

The strongest motivation for requiring an energy resolution of $\Delta E \leq 2$ eV is provided by the sensitivity to detecting narrow emission lines in faint groups of galaxies. However, a resolution of 2 eV by itself also provides access to an array of spectroscopic diagnostics that will be a rich source of information on astrophysical sources of all kinds, in particular more nearby objects like supernova remnants, stellar coronae and accretion flows in X-ray binaries. Some of these diagnostics are shown in Figure 12, in terms of the required minimum resolving power versus photon energy. Also indicated in this figure is the predicted performance of two proposed implementations of the 2 eV resolution requirement: a Superconducting Tunneling Junction array (STJ) with Fano-limited performance, and a Transition Edge Sensor micro-calorimeter (TES). A CCD-type Wide Field Instrument (WFI) yielding a field of view of 5 x 5 arcmin^2 at moderate energy resolution (~ 50 eV) completes the instrument suite.

4 Specific Science Examples

4.1 AGN versus starbursts at z = 1 – 4

In order to examine the sensitivity of XEUS for spectroscopic observations of high-redshift AGN and its ability to discriminate between AGN and starburst emission, spectra of a composite starburst galaxy plus a heavily absorbed AGN (Fig. 13) have been simulated. It was assumed that at lower energies only emission from the starburst is seen, which was modelled as a thermal gas at kT = 3 keV with 0.3 solar metallicity. At higher energies, the absorbed AGN is visible with a strong (EW = 1 keV) Fe-K line, probably due to transmission through, and reflection by, absorbing material with $N_H = 10^{24}$ cm^{-2}. Such a model is similar to that of nearby galaxies such as NGC 6240, NGC 4945, and MKN 3. The intrinsic source luminosity was *conservatively* normalised to the 0.1 – 2.0 keV luminosity of NGC 6240 (2 x 10^{42} erg s^{-1}). Figures 14 and 15 clearly demonstrate that XEUS1 will allow a detailed study of such sources around z = 1, but that XEUS2 is required to perform spectroscopy at $z \gg 1$. It should be noted that such results have been obtained assuming a rather conservative cosmology with $H_0 = 50$ km s^{-1} Mpc^{-1} and $q_0 = 0$.

Such X-ray spectra would be the only way to obtain direct proof of the existence of dust-enshrouded AGN at high redshift. If detected, they would allow the starburst versus AGN contribution to be directly disentangled. If undetected, they would provide strong limits on the AGN contribution. This would have important consequences on the star formation and ionisation histories of the Universe.

4.2 XEUS deep field

The right panel of Figure 15 shows the spectrum of the same source at a redshift of 8 obtained with a 10^6 s exposure time.The Fe-K line, if present, could be clearly detected and, as a consequence, the redshift directly measured without optical/IR spectroscopy. Several tens of AGN with $z \geq 3$ are expected in such a deep field (see right panel of Fig. 4). We stress that such exciting results are obtained because, even though the sources are weak, the high redshifts of the sources 'shift' the strong Fe-K line and absorption features expected from these sources into the low-energy band (< 2 keV) where XEUS has the highest effective area.

4.3 Resonance absorption lines from warm and hot gas

XEUS will be the first X-ray observatory capable of detecting resonance absorption lines for a wide range of objects. This results from the unique combination of large effective area and high spectral and spatial resolutions. The use of resonance absorption lines can be applied to several problems, as it is in optical/UV astronomy. Resonance absorption lines are generally detectable at much lower column densities than absorption edges (which do not require high-resolution spectroscopy), and therefore can trace gas that is too tenuous to be seen by other means.

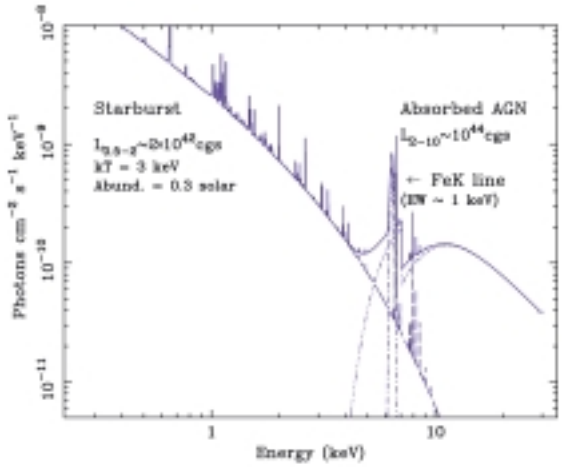

Figure 13. Model used in the simulations shown in Figures 14 and 15.

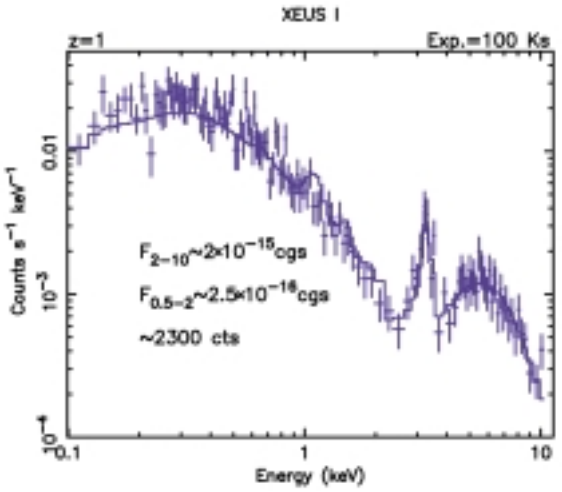

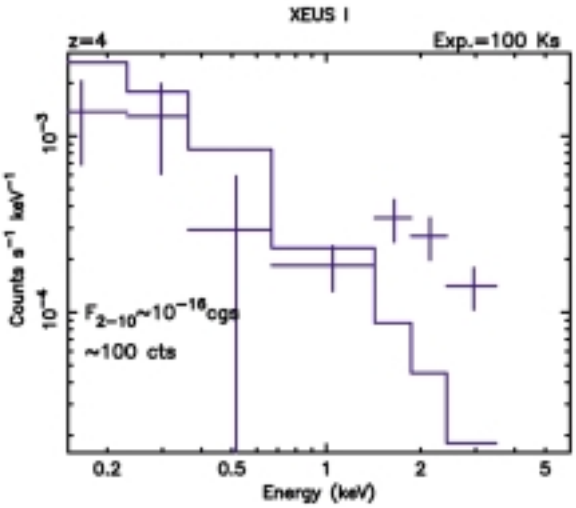

Figure 14. XEUS1 spectra at z = 1 (left) and z = 4 (right). These illustrate the limits of the XEUS1 configuration.

Figure 15. XEUS2 spectra at z = 4 (left) and z = 8 (right). These illustrate that, with a WFI deep-field exposure of 10^6 sec, spectra of sources at z = 8 could be obtained and their Fe-K line characterised.

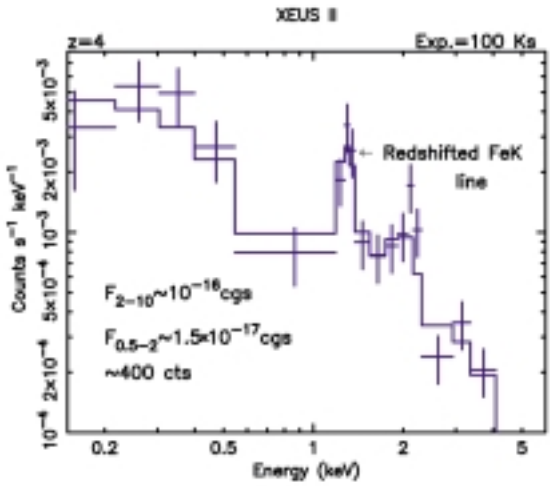

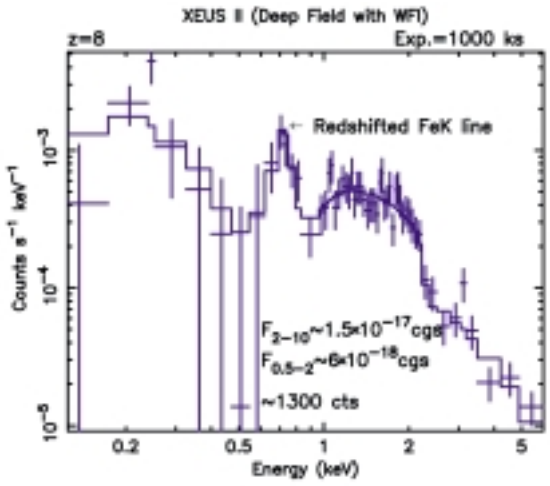

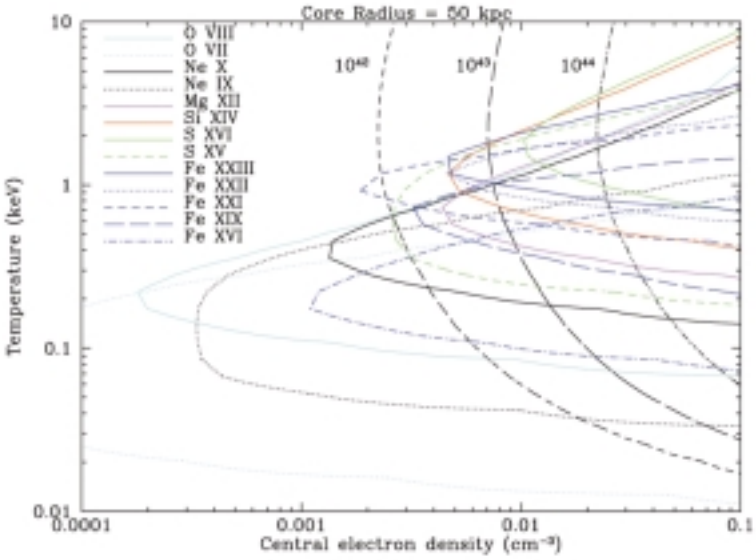

Figure 16. Contours corresponding to an EW limit of 0.2 eV for an absorber at z = 1 and 1/3 solar metallicity, for some prominent transitions. The "vertical" lines show continuum emissivities from the absorbing gas in the 0.1 - 2.4 keV energy range, assuming a standard ß = 2/3 profile model.

Intervening hot/warm gas clouds along the line of sight towards distant background sources will produce resonance absorption lines. Among the main astrophysical problems that can be addressed with the study of these X-ray absorbers are:

- The use of absorber number counts and their redshift dependence to test models of large-scale structure formation.
- Determination of the temperature distribution of baryons in the Universe.
- Determination of metallicities of the absorbers, in particular the [O/Fe] ratio to infer the relative rates of type-I and type-II supernovae.
- Determination of the redshift evolution of parameters such as number counts, gas temperatures, and metallicities.
- Where the emitting gas is also seen in absorption, use both emission and absorption to infer the distance, and therefore measure key cosmological parameters (see, for example, Ref. 23).

X-ray emission from the hot Universe can only be seen in structures that are sufficiently dense and hot. Resonance absorption lines can trace much more tenuous and warm gas[19,32] and therefore can be instrumental in tracing the majority of the baryons in the Universe. The detection of resonance absorption lines requires the presence of a bright background source. Around a given line of sight, the number of absorption systems per unit redshift scales as $N_{com}R^2(1+z)/(1+2q_0z)^{1/2}$, where N_{com} is the co-moving number density of absorbing clouds and R their size. Therefore, in the absence of evolution, absorption-line studies sample the region around the line of sight with no strong redshift dependence. Detection of resonance absorption lines out to any redshift is only subject to the existence of a sufficiently bright background sources.

The expected equivalent widths of the most prominent absorption lines produced by groups and clusters of galaxies range from a few tenths of eV to

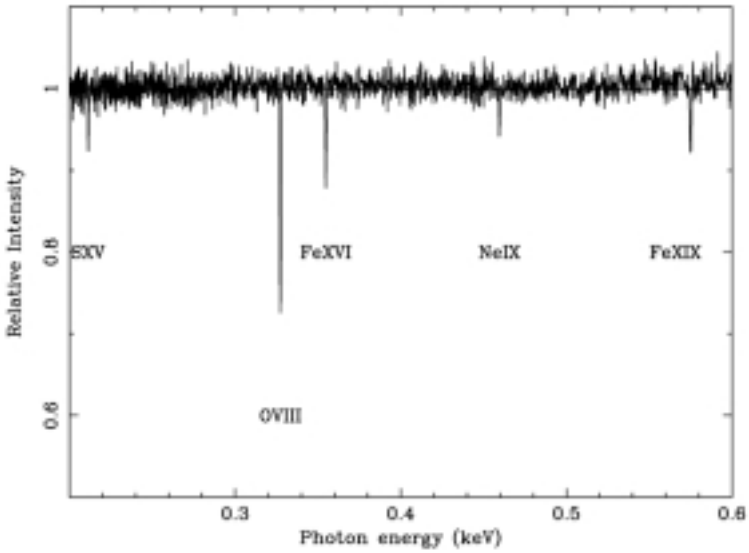

Figure 17. Absorption-line spectrum towards a 10^{-12} erg cm^{-2} s^{-1} AGN (0.5 - 2 keV) observed for 100 ksec with XEUS2/STJ. The line of sight is assumed to cross a small group with a 0.1 - 2.4 keV luminosity of 10^{42} erg s^{-1} at z = 1 with a core radius of 50 kpc. For a 10^{-13} erg cm^{-2} s^{-1} background source, the O VIII line is clearly detected.

a few eV (see Refs. 23 and 39). For a typical power-law photon index of 1.7 and absorbing column of 2 x 10^{20} cm^{-2} for the background source, most of the sensitivity of the XEUS/STJ combination is in the 0.2 – 1.0 keV energy range. With a 100 ksec observation, a signal-to-noise ratio >10 spectrum (the minimum to detect narrow absorption features) over the desired spectral region is obtained for a source with 0.5 – 2 keV flux of < 10^{-13} erg cm^{-2} s^{-1} with XEUS2. With this sensitivity, absorption lines as weak as 0.2 eV EW can be detected in the spectrum of any sufficiently bright background source.

Simulations of collisionally excited gas in ionisation equilibrium at different temperatures were performed to investigate what type of structures can be detected using XSTAR. Figure 16 shows the EW = 0.2 eV limit for a gas volume with a King profile with a core radius of 50 kpc and ß = 2/3 at z = 1 (metallicity 0.3 solar), together with contours showing gas-emission luminosities of 10^{42}, 10^{43} and 10^{44} erg s^{-1}. As noted in Reference 19, the O VII line is a very good tracer of warm (10^5 – 10^6 K) gas. Poor groups (~ 10^{42} erg s^{-1}) are clearly detectable against a bright source. A particular example is shown in Figure 17.

Cosmological models predict a sky-covering fraction of hot gas in groups and clusters of ~1, and therefore absorption systems will be found routinely towards all distant background sources. However, experience accumulated from the optical/UV absorption-line studies demonstrates that even the deepest galaxy surveys would not be expected to have more than one absorber per 10 to 100 lines of sight. Instead, between 10 and 100 absorbers are detected as Ly α absorbers per line of sight.

Finally, we would remark that resonance absorption lines caused by the warm/hot gas intrinsic to the AGN themselves will also be detectable with XEUS. This opens up the possibility to study the various components of the absorbing gas intrinsic to AGN, their kinematical state and abundances, etc.

Probing the early Universe using gamma-ray-burst afterglows

XEUS will provide the potential for observing the afterglows of gamma-ray bursts (GRBs).This will allow the study of galaxy, star and heavy-element formation at z > 3. Following BeppoSAX observations[9,35], it is known that GRBs are at cosmological distances[26] and amongst the most luminous objects in the Universe. During the explosion, their inferred luminosity can reach 10^{54} erg s^{-1}. The energy output is, however, not limited to the few seconds of the burst, but continues for months after it. In this phase, GRBs produce a huge amount of ionising flux, which interacts with the nearby environment. If GRB progenitors are massive stars, they will have had no time to move away from their formation site. GRBs will then go off in a mass-rich environment, with a typical size of ORDER 1 pc. Estimates of the expected Fe line intensity have been carried out[5]. The intensity appears too faint to be detected by the next-generation X-ray missions (e.g. XMM,

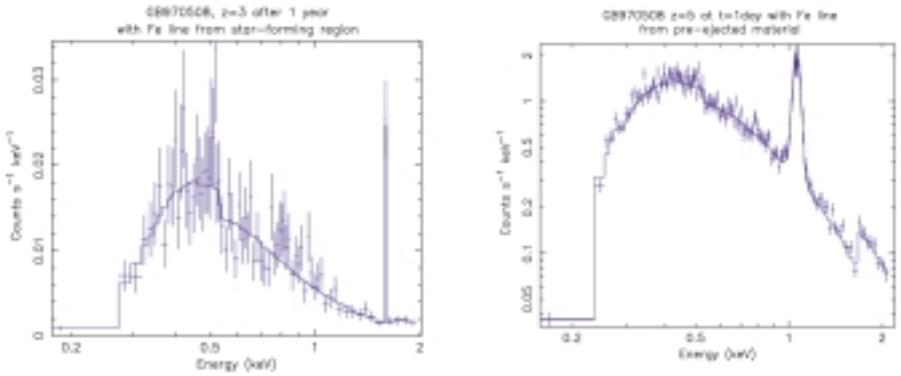

Figure 18. Left: A XEUS simulation of an Fe line from a star-forming region (assuming solar-like abundances) embedding a GRB at z = 3 with an Fe line flux of 2 x 10^{-9} photons cm^{-2} s^{-1}. The GRB X-ray continuum is like that of GRB 970508 redshifted to z = 3 and observed 1 year after the GRB (a 0.1 - 2 keV flux of 5 x 10^{-17} erg cm^{-2} s^{-1}). An exposure time of 100 ksec was assumed.
Right: A XEUS simulation of an Fe line from a pre-ejected medium in a GRB 970508-like event at z = 5 with an Fe line flux of 5 x 10^{-7} photons cm^{-2} s^{-1}. The event is observed 1 day after the GRB with an exposure of 20 ksec. The 0.1 - 2.0 keV continuum flux is 5 x 10^{-15} erg cm^{-2} s^{-1}.

Figure 19. Absorption features imprinted on the spectrum of a GRB by its host, a star-forming galaxy at z = 5. Absorption of N_H = 6 x 10^{22} cm^{-2}, solar abundances and an exposure of 50 ksec were assumed. The GRB X-ray continuum is similar to that of GRB 990123 redshifted to z = 5 and observed 12 h after the GRB.

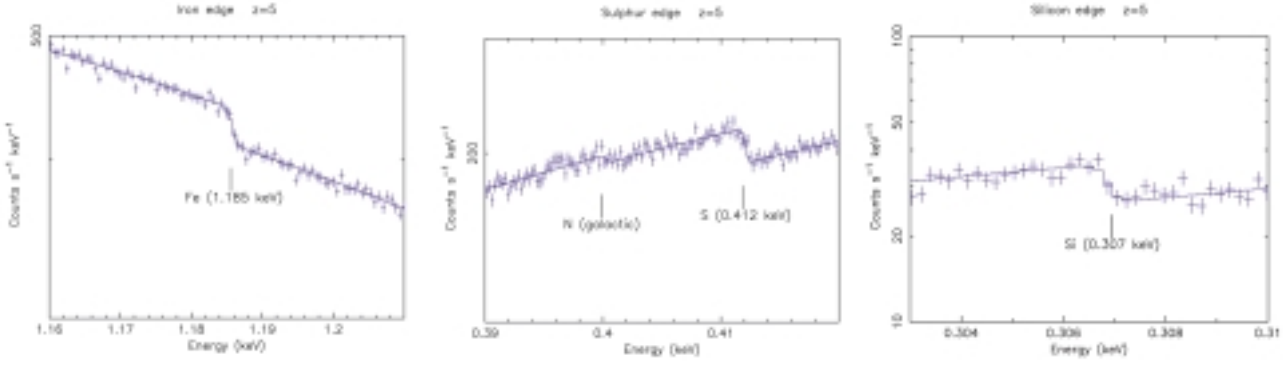

Astro-E), unless a GRB is unusually near and the medium has an Fe abundance significantly larger than the solar value. With XEUS, it will be possible to probe these regions up to z = 3 – 5, even for a chemical composition close to solar (Fig. 18).

A GRB may be embedded in a much closer and denser medium pre-ejected by the progenitor, possibly a supernova, as suggested by the tentative evidence of redshifted Fe-K lines observed in two X-ray afterglows[36,46]. In this case, it will be possible to study the metal enrichment processes and the properties of progenitors at much higher redshift, z > 5 (Fig. 18).

Due to their high luminosities, GRB can also be used as very bright background objects to study the state and composition of absorbing systems along the line of sight. The case of resonance absorption lines from a warm gas has been illustrated in the previous section. In Figure 19, we show an example with a local N_H = 6 x 10^{22} cm^{-2} at z = 5 from a cold medium in the parent galaxy. The abundances and ionisation states of the heavy elements can be determined precisely. Even with an absorption column density 10 times lower, most of the element abundances can be measured with an uncertainty of 10 – 30%.

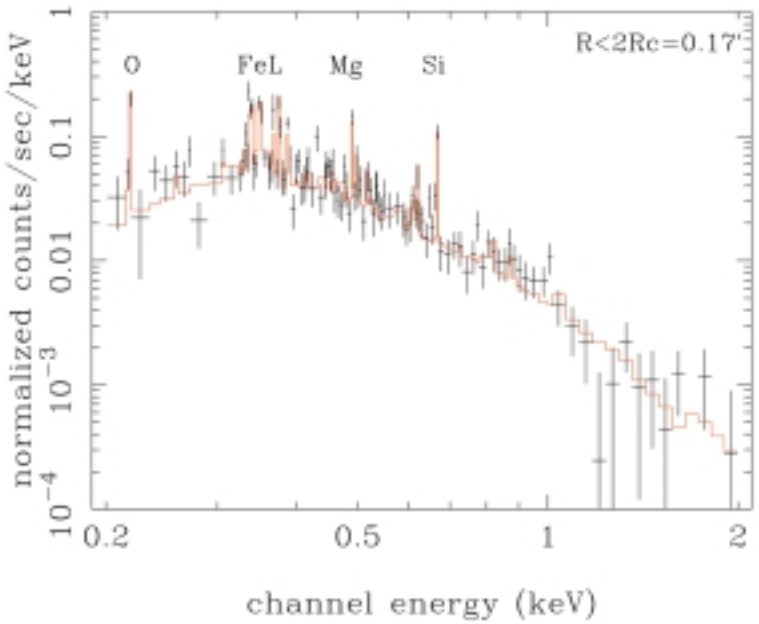

Figure 20. Simulated spectra of a very high redshift group (kT = 1.5 keV) located at z = 2. The abundances and temperature can be measured with accuracies of ± 3, 10 and 20% for the kT, Fe, and O abundances, respectively.

XEUS observations of the most distant galaxy systems

To illustrate the potential of XEUS to study the formation of the large-scale structure and galaxy clusters, we concentrate on simulations of observations of distant galaxy groups. In the standard cosmological models, these groups are the first emerging massive objects, with masses of the order of 10^{13} $M_\odot$. The precise epoch of their first formation depends very critically on the adopted cosmological model and is therefore not well known. Within the cosmological parameter range allowed by current observational constraints,

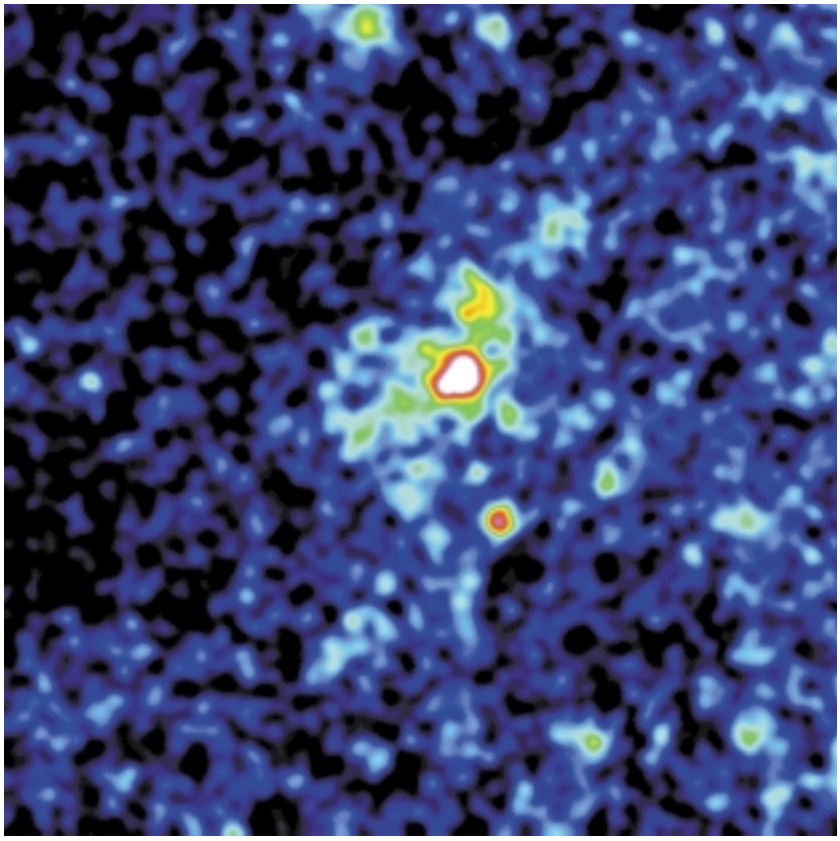

Figure 21. Simulated image of a Hickson-type group with L_x = 10^{43} erg s^{-1} at z = 2 with parameters similar to the model of Fig. 20. An angular resolution of 5 arcsec HEW was assumed.

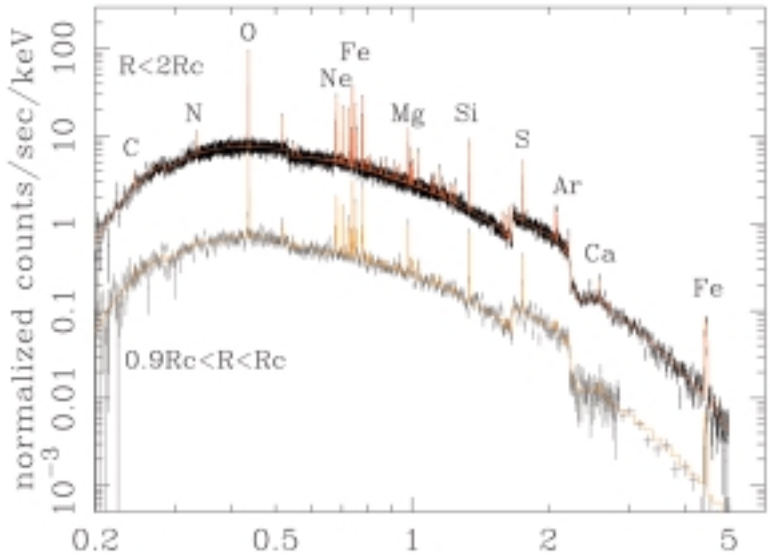

Figure 22. Simulated XEUS2 spectra (100 ksec) of a z = 0.5 cluster with a moderate bolometric luminosity of 1.6 x 10^{44} erg s^{-1}. Top: emission from within two core radii (R_c). Note the highly significant detection of lines from astrophysically abundant elements (the Fe abundance is measured to an accuracy of 2%, C to 30% accuracy). Bottom: The emission from an annulus of width Δ(R) = 0.01 R_c located at 0.1 R_c from the centre. Again, the distribution of elements can be accurately determined.

the first groups should be present at z = 2 – 3, but could be found at redshifts as large as 5 in the low-Ω models. Massive clusters are expected to appear at significantly lower redshifts. Therefore, the study of groups will provide deep probes into the Universe.

Small groups with typical masses around 10^{13} $M_{\odot}$ have sufficiently deep gravitational potential wells that the intra-group gas is heated to 'X-ray temperatures' during their formation and remains essentially trapped in the potential. Thus, galaxy systems with dark-matter halos and with total masses of this order form the smallest laboratories for studying the hot thermal intergalactic gas. Conservative estimates with preferred cosmological models predict space densities of such groups at z = 1.5 – 2 (and Δ z = 1) of about 1 per several 10 arcmin^2. Thus, such groups will be serendipitously found in fields of normal XEUS observations.

Figure 20 shows a simulated spectrum of a typical group at z = 2 in a 200 ksec observation with the NFI1 instrument on XEUS2. Emission lines of Fe and the major ALPHA-elements are clearly visible in the spectrum. The temperature can be determined with an accuracy of better than ± 3%, and the abundances of Fe and O to better than 10% and 20%, respectively. Figure 21 shows an image as expected for such an observation, where a nearby compact group observed with ROSAT has been used as a template and smoothed to have an angular resolution of 5 arcsec HEW. This resolution is sufficent to resolve features on a physical scale of 40 – 50 kpc (depending on the cosmological model), which is enough to resolve the core radius, the radial structure and major features of substructure. At the higher resolution of 2 arcsec, even details in the core region can be resolved.

For comparison, Figure 22 shows the spectrum of a typical poor cluster with a luminosity of 1.6 x 10^{44} erg s^{-1} and a temperature of 3 keV at the moderate redshift of 0.5. In this case, the spectral lines of all the astrophysically important and abundant elements can be resolved and their spatial distribution measured. Such observations will allow the study of the element production by various types of supernovae and the enrichment by stellar winds in unprecedented detail.

4.6 Galaxy formation: outflowing hot gas

The formation of galaxies, which occurs at moderate and high redshifts (z > 1), is accompanied by a copious outflow of hot gas from supernovae. In the case of disk formation, the outflow is preferentially perpendicular to the disk and along the minor axis (as in the small local starburst galaxy M 82). Depending on the initial mass of the disk, such starburst activity may effectively destroy the disk or render it incapable of further star formation by ejecting the bulk of the hydrogen from the interstellar medium. These galactic outflows are responsible for the chemical enrichment and heating of the intergalactic medium and therefore also influence the subsequent evolution of galaxies. Observations at X-ray wavelengths are therefore very important in the study of galaxy formation and the formation of groups and

clusters. By performing spectroscopy of this hot gas at moderate to high redshift, XEUS will permit insights into the process of galaxy formation and subsequent evolution. Measurements of abundances of the heavy elements in this gas will allow constraints to be placed on the initial mass function and star-formation rates. These measurements will be complementary to those of the abundances in the gas clouds that are responsible for the quasar optical absorption lines.

NGC 3256 is a starburst galaxy, probably typical of those rapidly forming stars at high redshift. Simulations of the spectrum of such a galaxy moved to z = 2 show that XEUS observations will allow the precise measurement of abundances in the outflowing gas. This redshift was chosen since the peak in star-forming activity in the Universe probably occurred at $z \geq 2$ (Ref. 24).

4.7 Stellar astronomy

The large effective area of the XEUS configuration provides unique opportunities for stellar X-ray astronomy. The high sensitivity means that solar-like X-ray emission can be detected out to distances of a few kiloparsecs, ignoring the effects of interstellar absorption. As a consequence, large samples of truly solar-like stars become amenable for study. For example, at the distance of M 67, an old open cluster with an age similar to that of the Sun, a limiting X-ray luminosity of 10^{26} erg s^{-1} can be reached, implying that solar minimum X-ray emission levels can be detected. This is particularly relevant for a study of activity cycles in other solar-like stars, since in the Sun the solar cycle is most easily detectable in the X-ray domain. In addition, the XEUS sensitivity is so large that in nearby open clusters such as the Hyades and Pleiades virtually all cluster stars will be detected as X-ray sources, and the X-ray-brightest cool stars can even be detected in nearby galaxies such as the Large Magellanic Cloud and the Andromeda Nebula. Searches for stellar X-ray emission can therefore be carried out over a significant fraction of the Galaxy.

Figure 23. Left: A simulated XEUS1/STJ spectrum of AR Lac. An exposure time of 100 sec was used. A similar quality spectrum is expected in only 20 sec with XEUS2. Centre: Details of the Fe-L region from the AR Lac simulation. Right: The spectral region near O Ly-α with line identifications. The simulation shows how clearly the properties of this astrophysically important line can be measured, even on such a short time scale.

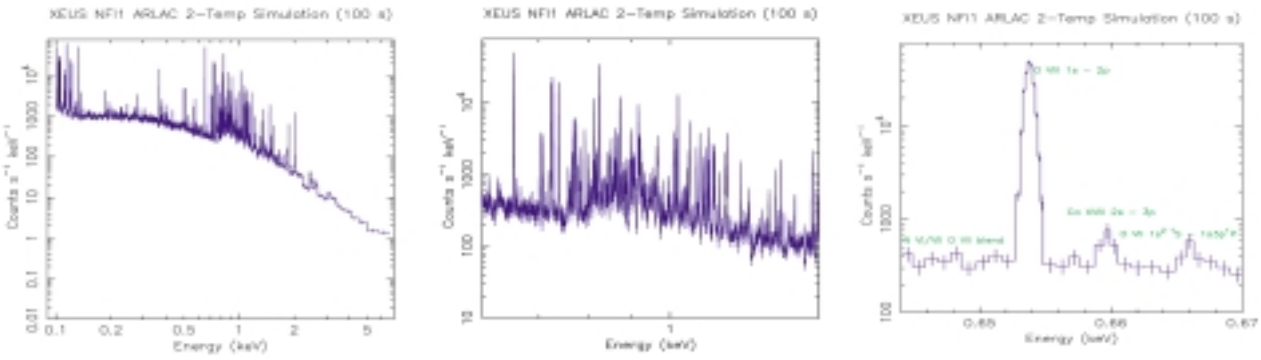

X-ray images of the Sun obtained with YOHKOH and SOHO have shown that hot plasma trapped in closed magnetic loops provides almost all of the X-ray emission from the solar corona. While the X-ray emission from such loops is usually ëquietí, i.e. not strongly variable over the dynamical loop time scales, sometimes restructuring of such magnetic loops gives rise to intense outbursts of radiation in the form of flares. On other stars, flares much more intense than those occurring on the Sun are observed and, again, the disruption of magnetic structures is thought to be responsible for the observed emission. Time-resolved high-resolution spectroscopy is required to understand and analyse the physics of such giant stellar flares. The potential of XEUS to perform such studies is illustrated by simulations of a 100 sec exposure of the nearby RS CVn system AR Lac. This system contains a G2 IV star and a K0 IV star in a two-day orbit. The simulations shown in Figure 23 are based on the results of ASCA observations and show the rich line-dominated spectra. The large area of XEUS means that a sufficient number of counts are obtained so that the temperature, density, chemical abundance and velocity distribution of the emitting plasma can be measured on very short time scales. This will allow the study of the evolution of these basic physical parameters during typical stellar flares with an accuracy only previously achievable with solar flares. From such data, astrophysicists expect new insights into the physical mechanism responsible for powering the most intense stellar flares and a detailed comparison with those observed on the Sun.

Conclusion

XEUS is an ambitious endeavour to take the next step forward in high-energy astrophysics in partnership with the International Space Station after the current two great observatories XMM-Newton and Chandra have completed their operational lives. Scientifically, it aims for the study of some of the faintest and youngest objects in our Universe through unparalleled spectral sensitivity. Technically, the recently completed industrial concept study; which involved an analysis of the mission scenario, Space Station interfaces and spacecraft system drivers, has clearly shown the feasibilty of the overall mission design.

ESA's Astronomy Working Group (AWG), at its meeting on 20-21 September 1999 [ASTRO(99)13], concluded that the XEUS mission is of the highest scientific quality. In particular, it felt that further 'technological and system studies are essential to continue over the next few years to elaborate in more detail the technology drivers and implementation scenarios'. This approach was endorsed by ESA's Space Science Advisory Committeee (SSAC) at its meeting on 21 September 1999 [SSAC/MIN/91].

References

1. Arnaud M., Rothenflug R., Boulade O., Vigroux L. & Vagioni-Flam E. 1992, A&A 254, 49.
2. Baudry A., 'On the Imaging Efficiency, Speed, and Sensitivity of Millimetre Arrays', Proc. ESO Astrophysics Symposium 'Science with Large Millimetre Arrays', held in Garching, 11-13 December 1995, Ed. P.A. Shaver (Springer).
3. Blain A.W. et al., 1999, MNRAS 302, 632.
4. Böhringer H., Guzzo L., Collins C.A. et al. 1998, The Messenger 94, 21.
5. Boettcher M., Dermer C.D., Crider A.W. & Liang E.P. 1999, A&AS 138, 543.
6. Cen R. & Ostriker J. 1999, ApJ 514, 1.
7. Comastri A. et al. 1995, A&A 296, 1.
8. Cooray A.R. 1999, A&A 348, 31.
9. Costa E. et al. 1997, Nature 387, 783.
10. Donahue M. et al. 1999, Pre-print (Astro-ph 9906295).
11. Fabian A.C., Barcons X., Almaini O. & Iwasawa K. 1998, MNRAS 297, L11.
12. Fabian A.C. et al. 1999, In preparation.
13. Gendreau K. et al. 1995, PASJ 47, 5.
14. Haiman Z. & Loeb A. 1999, ApJ 521, L9.
15. Hasinger G., in 'The X-ray Background', Barcons X. & Fabian A.C. (Eds.), Cambridge University Press, p. 229.
16. Hasinger G. et al. 1993, A&A 275, 1.
17. Hasinger G. et al. 1998, A&A 329, 495.
18. Hasinger G. et al. 1999, Highlights in X-ray Astronomy, Proc. Workshop in honour of J. Trümper's 65th birthday, Garching, June 1998.
19. Hellsten U., Gnedin N. & Miralda-Escudé J. 1998, ApJ 509, 56.
20. Henry J.P., Briel U.G. & Böhringer H. 1998, Sci. Am. 279, 52.
21. Hughes J. et al. 1998, Nature 394, 241.
22. Jakobsen P. 1998, ESA's Involvement with NGST, in: 'The Next Generation Space Telecope', Proc. 34th Liège International Astrophysics Colloquium, ESA SP-429.
23. Krolik J. & Raymond J. 1988, ApJ 335, L39.
24. Madau P. et al. 1996, MNRAS 283, 1388.
25. Marzke R.O. et al. 1998, ApJ 503, 617.
26. Metzger M.R. et al. 1997 Nature 387, 878.
27. Maiolino R. et al. 1998, A&A 338, 781.
28. Miyaji T. et al. 1998a, A&A 334, 13.
29. Miyaji T., Hasinger G. & Schmidt M. 1998b, Highlights in X-ray Astronomy, Proc. Workshop in honour of J. Trümper's 65th birthday, Garching, June 1998.
30. Mushotzky R. & Scharf C. 1998, ApJ 482, L13.
31. Parmar A.N. et al. 1999, A&A 345, 611.
32. Perna R. & Loeb A. 1998, ApJ 503, L135.
33. Pettini M. 1998, ApJ 508, 539.
34. Pilbratt G. 1998, The FIRST ESA Cornerstone Mission. in 'Space Telescopes and Instruments V', SPIE 3356, 452.
35. Piro L. et al. 1996, A&A 329, 906.
36. Piro L. et al. 1999, ApJ 514, L73.
37. Ponman T.J., Bourner P.D.J., Ebeling H. & Böhringer H. 1996, MNRAS 283, 690.
38. Roche N. et al. 1996, MNRAS 282, 820.
39. Sarazin C. 1989, ApJ 345, 12.
40. Schmidt M., Schneider D.P. & Gunn J.E. 1995, AJ 110, 68.
41. Setti G. & Woltjer L. 1989, A&A 224, L21.
42. Silk J. & Rees M. 1998, A&A 331, L1.
43. Tegmark M. et al. 1997, ApJ 474, 1.
44. Vignati P. et al. 1999, A&A 349, L57.
45. White S.D.M., Navarro J.F., Evrard A.E. & Frenk C.S. 1993, Nature 366, 429.
46. Yoshida A. et al. 1999, A&AS 138, 433.